Tissue- and Age-Dependent Differences in the Complexation of Cadmium and Zinc in the Cadmium/Zinc Hyperaccumulator *Thlaspi caerulescens* (Ganges Ecotype) Revealed by X-Ray Absorption Spectroscopy[1][w]

Hendrik Küpper*, Ana Mijovilovich, Wolfram Meyer-Klaucke, and Peter M.H. Kroneck

Universität Konstanz, Mathematisch-Naturwissenschaftliche Sektion, Fachbereich Biologie, Postfach M665, D–78457 Konstanz, Germany (H.K., P.M.H.K.); University of South Bohemia, Biological Faculty, Branišovská 31, CZ–370 05 České Budějovice, Czech Republic (H.K.); and EMBL Outstation Hamburg c/o Deutsches Elektronen-Synchrotron, Notkestrasse 85, D–22603 Hamburg, Germany (A.M., W.M.-K.)

Extended x-ray absorption fine structure measurements were performed on frozen hydrated samples of the cadmium (Cd)/zinc (Zn) hyperaccumulator *Thlaspi caerulescens* (Ganges ecotype) after 6 months of Zn^{2+} treatment with and without addition of Cd^{2+}. Ligands depended on the metal and the function and age of the plant tissue. In mature and senescent leaves, oxygen ligands dominated. This result combined with earlier knowledge about metal compartmentation indicates that the plants prefer to detoxify hyperaccumulated metals by pumping them into vacuoles rather than to synthesize metal specific ligands. In young and mature tissues (leaves, petioles, and stems), a higher percentage of Cd was bound by sulfur (S) ligands (e.g. phytochelatins) than in senescent tissues. This may indicate that young tissues require strong ligands for metal detoxification in addition to the detoxification by sequestration in the epidermal vacuoles. Alternatively, it may reflect the known smaller proportion of epidermal metal sequestration in younger tissues, combined with a constant and high proportion of S ligands in the mesophyll. In stems, a higher proportion of Cd was coordinated by S ligands and of Zn by histidine, compared with leaves of the same age. This may suggest that metals are transported as stable complexes or that the vacuolar oxygen coordination of the metals is, like in leaves, mainly found in the epidermis. The epidermis constitutes a larger percentage of the total volume in leaves than in stems and petioles. Zn-S interaction was never observed, confirming earlier results that S ligands are not involved in Zn resistance of hyperaccumulator plants.

Heavy metals such as copper, manganese, nickel (Ni), and zinc (Zn) are well known to be essential microelements for the life of plants, and recently, even cadmium (Cd) was found to act as the active center of a plant enzyme (Lane and Morel, 2000). On the other hand, elevated concentrations of these metals induce inhibition of plant metabolism, leading to various effects depending on the metal applied, the type of affected plant, and the environmental conditions during the stress (for review, see Clijsters and Van Assche, 1985; Fernandes and Henriques, 1991; Barón et al., 1995; Prasad and Hagemeyer, 1999).

Plants developed a number of strategies to resist the toxicity of heavy metals, such as efflux pumps (van Hoof et al., 2001), complexation of heavy metals inside the cell by strong ligands such as phytochelatins (for review, see Cobbett and Goldsbrough, 2002) or His (Krämer et al., 1996), and several more mechanisms (Maeda and Sakaguchi, 1990; Prasad and Hagemeyer, 1999). Plants that actively prevent metal accumulation inside the cells are called excluders. These represent the majority of metal-resistant plants (Baker, 1981). Other resistant plants deal with potentially toxic metals in just the opposite way, i.e. they actively take up metals and accumulate them. The active accumulation in the aboveground parts of hyperaccumulator plants provides a promising approach for both cleaning anthropogenically contaminated soils (phytoremediation) and for commercial extraction (phytomining) of metals from naturally metal-rich (serpentine) soils (McGrath et al., 1993, 2002). These plants, which have been named "hyperaccumulators" (Brooks et al., 1977), are able to accumulate several percent metals in the dry weight of their aboveground parts. By now, more than 400 species of hyperaccumulators for diverse metals have been identified, and 75% are Ni hyperaccumulators (Baker and Brooks, 1989; Brooks, 1998). In contrast, only 16 species of Zn hyperaccumulators have been found so far (Brooks, 1998), the best known of which is *Thlaspi caerulescens* J. & C. Presl. This species, and in particular the Ganges ecotype, is the first one that

[1] This work was supported by the European Community "Access to Research Infrastructure Action of the Improving Human Potential Programme" to the EMBL Hamburg Outstation (contract no. HPRI–CT–1999–00017), by the Deutsche Forschungsgemeinschaft, and by the Ministry of Education of the Czech Republic (grant nos. VS96085 and ME138).

[w] The online version of this article contains Web-only data.

* Corresponding author; e-mail Hendrik.Kuepper@uni-konstanz.de; fax 607–255–2459.

Article, publication date, and citation information can be found at http://www.plantphysiol.org/cgi/doi/10.1104/pp.103.032953.

has been shown to be also a true Cd hyperaccumulator (referred to as "French A" in Lombi et al., 2000), in the sense of accumulating more than 10,000 ppm Cd in the dry weight of its aboveground parts. Although Lombi et al. (2000) were the first to report that the Ganges ecotype accumulates many times more Cd than other *T. caerulescens* ecotypes, Robinson et al. (1998) had shown already that it generally accumulates Cd in its natural environment.

Several studies have shown that metal accumulation serves as a defense mechanism against herbivores and pathogens (Boyd, 1998). Pence et al. (2000) found that the increased uptake of Zn is because of a much higher expression level of specific Zn transport proteins. For understanding and finally further enhancing the mechanisms of hyperaccumulation, it is crucial to know whether the metals hyperaccumulated inside the cells are bound by strong specific ligands (Krämer et al., 1996), or whether they are only loosely associated with organic acids (Salt et al., 1999) that are always abundant in plant cell vacuoles. Especially for Cd but also for Zn, very little is known with regard to these questions in hyperaccumulator plants. Küpper et al. (1999, 2000) reported that the total sulfur (S) concentration in cells is lower than the Cd concentration and that there is no correlation between the concentrations of Zn and S. Clearly, the major ligands for both Cd and Zn in hyperaccumulator plants must be different from the phytochelatins known from normal plants (for review, see Cobbett and Goldsbrough, 2002). Further evidence to this end was obtained by Ebbs et al. (2002), who demonstrated that phytochelatin levels in both shoots and roots of Cd-accumulating *T. caerulescens* are lower than in the related nonaccumulator *Thlaspi arvense*. Finally, a number of recent studies have indicated that metal compartmentation is a key resistance mechanism. Metals were shown to be preferentially sequestered in compartments (vacuoles) and cell types (epidermal storage cells) where they do least damage to photosynthesis (Küpper et al., 1999, 2000, 2001; Frey et al., 2000; Psaras et al., 2000; Psaras and Manetas, 2001). When metal concentrations in hyperaccumulators, however, reach toxic levels, several additional resistance mechanisms may become activated. In the mesophyll of metal-stressed hyperaccumulator plants, an increase of the Mg content was found (Küpper et al., 2000, 2001), which was interpreted as a defense against the replacement of Mg^{2+} in chlorophyll by heavy metals (Küpper et al., 1996, 1998, 2002).

The method of extended x-ray absorption fine structure (EXAFS) is an element specific method and, therefore, particularly suited for analyzing the in vivo ligand environment of Cd and Zn in plants. Furthermore, in contrast to most other spectroscopic methods, it is applicable to intact frozen tissues, which was done first by Salt et al. (1995). In addition, EXAFS offers a much higher sensitivity compared with the main alternative method, NMR.

In the present study, EXAFS was used to investigate the ligand environment of both Zn and Cd in frozen hydrated tissues of *T. caerulescens* (Ganges ecotype). This ecotype of *T. caerulescens*, originally called "French A" (Lombi et al., 2000), has the highest known Cd hyperaccumulation capacity. Several tissues of different ages and with different metal treatments were analyzed to identify differences in metal coordination caused by aging, by differences in tissue function, and by different levels of Cd-induced stress. Model complexes were prepared as references.

RESULTS

Plant Growth and Metal Uptake

Plants treated with Cd^{2+} showed a reduced growth (shoot fresh weights after 12 weeks of growth: Zn-only plants, 5.32 [±1.60] g; 50 μM Cd, 1.08 [±0.18] g; 100 μM Cd, 0.50 [±0.14] g) and slight chlorosis compared with the plants grown only with Zn^{2+}, i.e. they suffered from pronounced but not lethal Cd toxicity. Although the Cd stress symptoms were pronounced in the exponential growth phase (see above), they diminished later, so that after half a year, much less difference was found between Cd-treated and Zn-only plants (data not shown). The metal analyses of digested samples showed not only the high capacity of Cd uptake of this plant species as published earlier (Lombi et al., 2000) but some further interesting aspects (Table I). For the first, the 100 μM Cd treatment did not yield a much higher Cd concentration in the plants than the 50 μM Cd treatment, i.e. the plants were able to down-regulate the Cd uptake. Much more surprisingly, the concentration of Zn was higher in the Cd-treated plants than in the controls. The effect was observable in all analyzed tissues

Table I. *Metal concentrations in the plant samples that were also analyzed by EXAFS*

To obtain representative datasets within the limited Synchrotron beam time, aliquots of samples from all plants of the same metal treatment (see "Materials and Methods") were mixed so that each EXAFS sample represented the average of four to eight plants.

Sample	Zn	Cd
	mg g⁻¹	
Young leaves, 100 μM Cd + 10 μM Zn	0.69	14
Mature leaves, 100 μM Cd + 10 μM Zn	0.94	21
Mature leaves, 50 μM Cd + 10 μM Zn	1.18	19
Senescent leaves, 100 μM Cd + 10 μM Zn	0.31	3.41
Dead leaves, 100 μM Cd + 10 μM Zn	0.79	12
Mature petioles, 100 μM Cd + 10 μM Zn	0.68	10
Senescent petioles, 100 μM Cd + 10 μM Zn	0.34	3.4
Mature stems, 100 μM Cd + 10 μM Zn	0.57	14
Senescent stems, 100 μM Cd + 10 μM Zn	0.27	3.9
Mature leaves, 0 μM Cd + 10 μM Zn	0.45	0.016
Mature petioles, 0 μM Cd + 10 μM Zn	0.27	0.004
Mature stems, 0 μM Cd + 10 μM Zn	0.065	0.005

(stems, petioles, and leaves) but was by far most pronounced in the stems, where the Zn concentration increased 10-fold as a response to Cd treatment (Table I).

EXAFS Measurements

Model Compounds

Several Cd and Zn model complexes were measured as "fingerprints" of the most important potential types of ligands in plants and, thus, facilitated the evaluation of the in vivo EXAFS data. The pH of the solutions of the model compounds resembled the pH of the compartment where these ligands are predominantly found in plant cells, e.g. acidic pH in case of the vacuole. The measurements have shown that these ligands yield clearly distinguishable XAS signals both for Cd (Fig. 1) and for Zn (see "Zn-standards.TIF" in the supplemental material and spectra published by Salt et al., 1999). White line intensity and position of maxima and minima especially change depending on coordination number, ligand type, and individual bond lengths. The differences were, however, much better visible and quantifiable (see below) in the EXAFS (Fig. 1, bottom) than in the XAS of the X-ray absorption near edge structure (XANES) region (Fig. 1, top). For all model compounds, the coordination numbers 4 to 6 were tested in the simulations of the data. For the aquo, citrate, and His complexes, the lowest fit index (FI) was found for a coordination number of six; for Cd-glutathione, the best result was obtained with a coordination number of five.

Plant Samples

In all samples obtained from plants grown on both Zn and Cd, the metal concentration was high enough to obtain EXAFS data with a good signal to noise ratio, as shown in Figure 2 for the Cd-EXAFS of a young leaf and in Figure 3 for the Zn-EXAFS of the same sample. Samples taken from different plant organs yielded clearly distinguishable XAS and EXAFS signals reflecting the different types of ligands involved in metal complexation in various parts of the plant investigated (Fig. 4; Tables II and III).

XAS averages over all metal environments present in the sample. To not bias any model, EXAFS data of all plant samples were tested for coordination numbers four to six. In all cases, the coordination number of six resulted in the lowest FI (data not shown). With this overall coordination number, the ratios of the potential ligands have been refined. During the refinement, the individual distances were allowed to vary. This provides an indicator for chemical correct results because any deviation from the typical individual bond length would identify models that are only mathematically correct. Table II summarizes the results from refining the EXAFS data with Excurve98

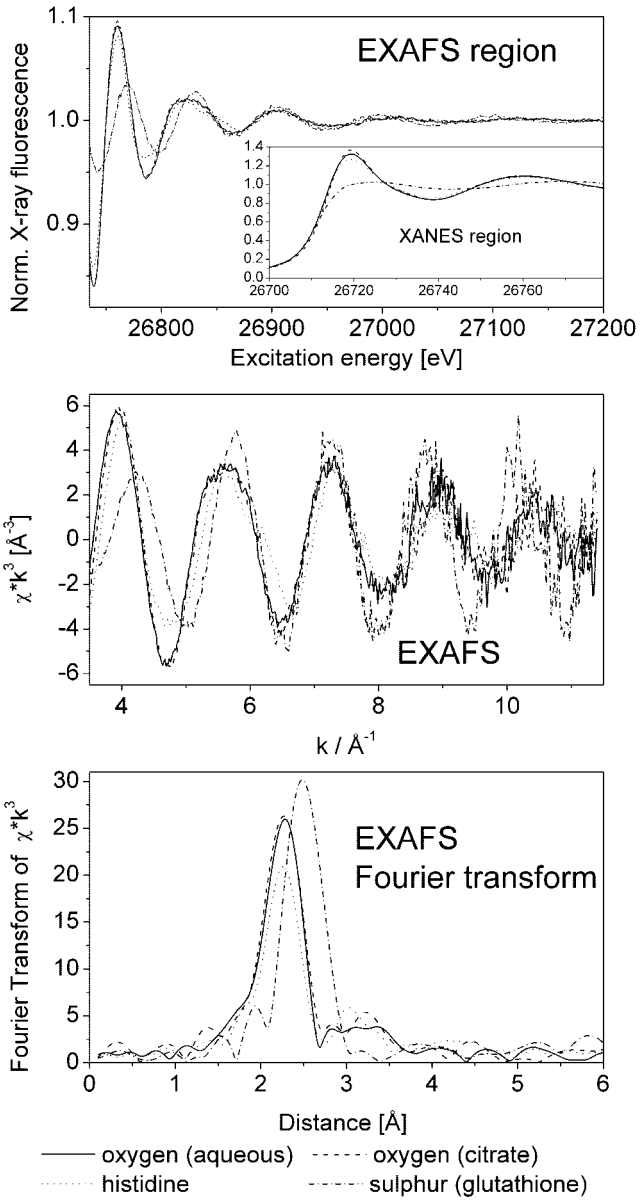

Figure 1. Comparison of Cd X-ray absorption spectroscopy (XAS) of different model compounds. Top, Raw data after normalization. Note that x-ray absorbance was measured as an excitation spectrum of x-ray fluorescence. Middle, Normalized EXAFS. Bottom, Fourier transform of the EXAFS.

and provide independent evidence for the presence of the ligands expected.

The results of the component analysis (CA) of the EXAFS region are shown in Table III. Obviously, both the CA and the refinement yielded qualitatively very similar results concerning the main ligands involved in metal complexation.

In all plant samples, an average first shell coordination of O/N with varying additions of S was detected as the main contribution. EXAFS analysis generally cannot discriminate between N and O ligation. However, His ligands can be identified via a specific

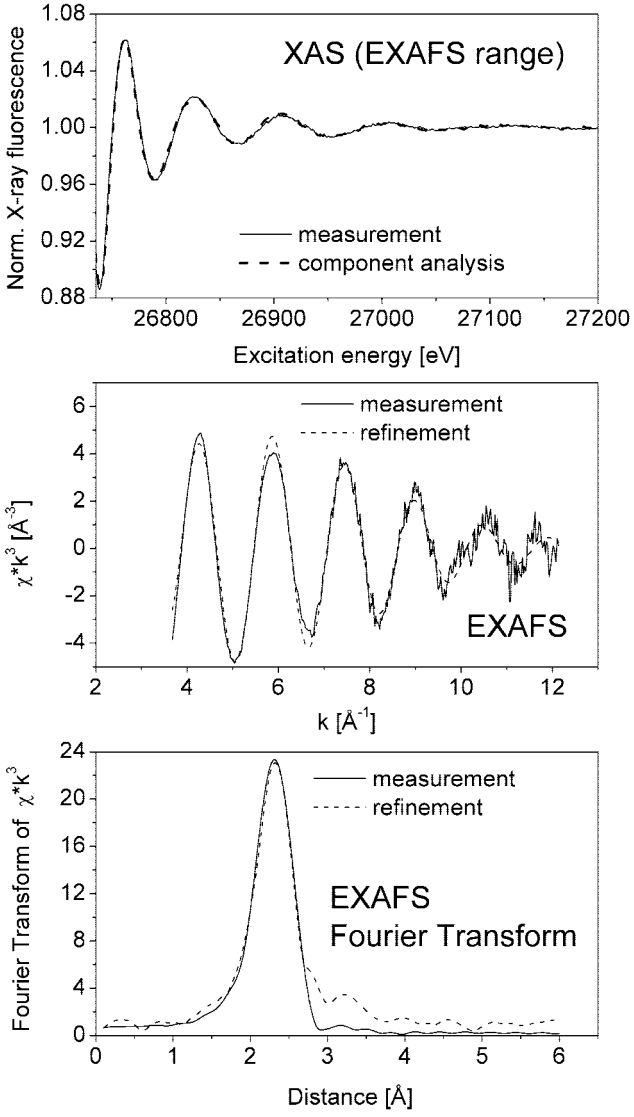

Figure 2. Typical example of data obtained by in situ x-ray absorbance measurements (Cd edge) of frozen hydrated *T. caerulescens* tissues. This example represents a measurement of Cd-EXAFS in a young leaf. Top, Raw data after normalization and fit with data sets of model compounds (see Table II). Note that x-ray absorbance was measured as an excitation spectrum of x-ray fluorescence. Middle, Normalized EXAFS and fit with theoretical model. Bottom, Fourier transform of the EXAFS and fits with theoretical model (done on normalized EXAFS) and fit with data sets of model compounds.

multiple scattering pattern they generate. Supported by data of the model compounds Cd-His and Zn-His, contributions at longer distances (Figs. 2 and 3, bottom) were attributed to the multiple scattering in the His ring. For Cd, however, this multiple scattering contribution is not that significant (for example, see Heinz et al., 2003). Thus, in the refinement, we did not further discriminate between nitrogen (N) and oxygen (O) donors. Therefore, for Cd, the His contribution was estimated only by the CA (Table III).

The ligand environment in the plant samples differed depending on the metal, the plant tissue, and the age of the tissue.

Metal-Specific Differences in Ligand Environment

In the case of Zn, the His contribution (multiple scattering contribution at around 3 and 4 Å) was much more pronounced than in the case of Cd (Figs. 2 and 3). No S ligands were detected around Zn,

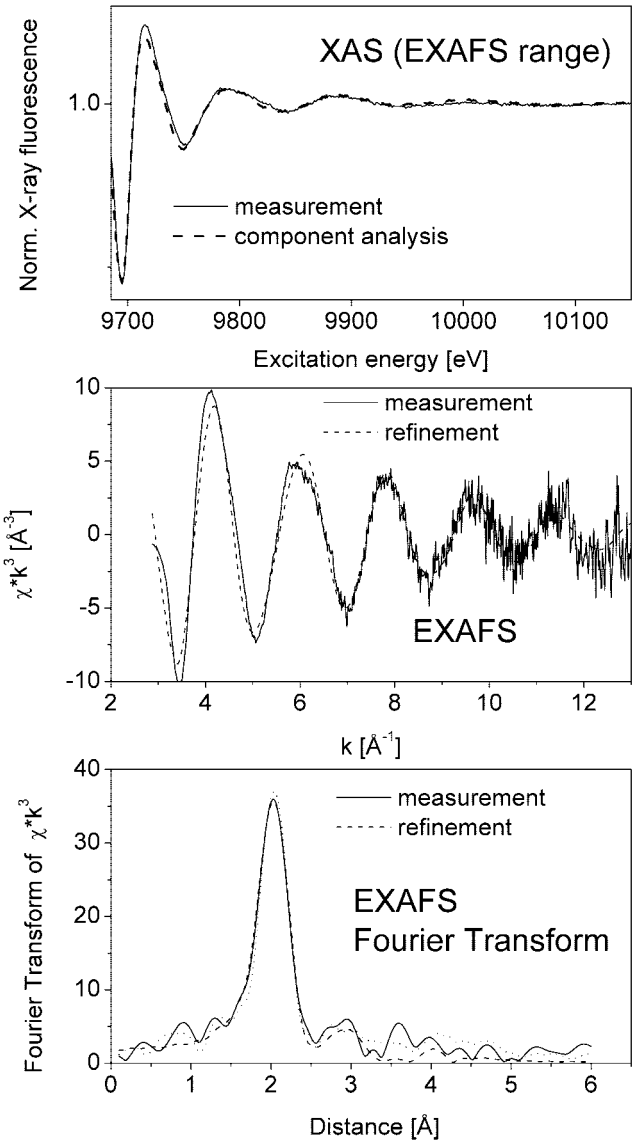

Figure 3. Typical example of data obtained by in situ x-ray absorbance measurements (Zn edge) of frozen hydrated *T. caerulescens* tissues. This example represents a measurement of Zn-EXAFS in a young leaf. Top, Raw data after normalization and fit with data sets of model compounds (see Table II). Note that x-ray absorbance was measured as an excitation spectrum of x-ray fluorescence. Middle, Normalized EXAFS and fit with theoretical model. Bottom, Fourier transform of the EXAFS and fits with theoretical model (done on normalized EXAFS) and fit with data sets of model compounds.

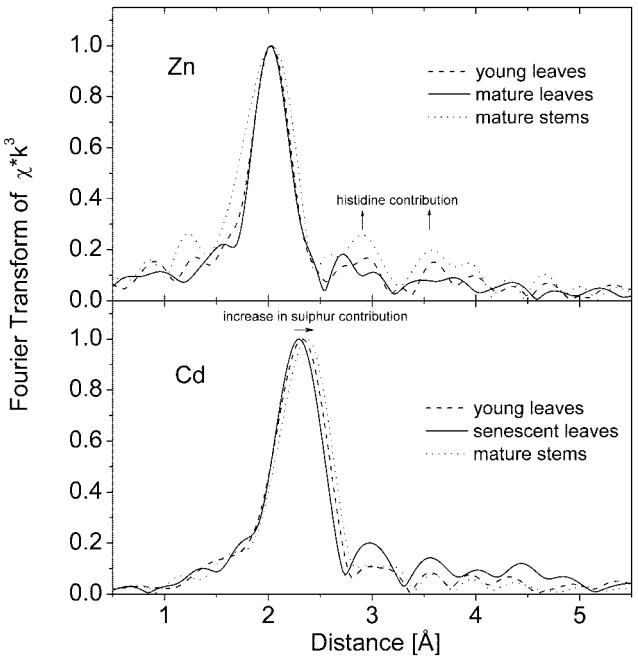

Figure 4. Examples of *T. caerulescens* EXAFS spectra (as Fourier transforms) showing differences in the ligand environment. All samples are from plants grown on 10 μM Zn and 100 μM Cd. Top, Zn edge. Bottom, Cd edge.

whereas a varying (see below) proportion of S ligands was found around Cd. The presence of Cd during plant growth did not lead to any association of Zn with S ligands (data not shown). Increasing the Cd concentration from 50 to 100 μM did not change the proportion of S ligands around Cd but increased the proportion of His ligands (Table III).

Age-Dependent Changes in Metal Speciation

The nature of Cd binding changed depending on tissue age (Tables II and III). In young leaves, around 25% of the Cd ligands were S ligands (e.g. phytochelatins, metallothioneins, and other Cys-rich peptides). The proportion of S ligands decreased with increasing leaf age; in senescent leaves, almost exclusively O ligands were found. The same trend was found comparing stems and petioles in the mature and senescent stage (Tables II and III). In addition, according to the CA (Table III), the proportion of His ligands increased from young to mature and from mature to dead leaves.

For Zn, there was no unidirectional trend. On the one hand, a higher proportion of strong ligands (here, only His) was present in young leaves compared with mature leaves, but this was found only in the CA (Table III), not in the refinement (Table II). On the other hand, there was an increase of His coordination from mature to dead leaves, i.e. the same effect that had been observed for His complexation of Cd. This was found both by the refinement (Table II) and the CA (Table III).

Tissue-Specific Differences in Metal Speciation

In mature stems, a large proportion of the metal was coordinated by specific ligands. His was predominant for Zn, and S ligands were predominant for Cd. In contrast, in mature and senescent leaves, both metals were predominantly bound by O ligands, which are rather weak and less specific. These O ligands could be either water or carboxyl groups of organic acids, such as citrate or malate.

DISCUSSION

The analyses of total metal content in the plant samples did not only confirm the high capacity of the Ganges ecotype of *T. caerulescens* for accumulating Cd (Lombi et al., 2000, 2001) but showed that at least in this ecotype, Zn and Cd uptake are interacting in an unusual way. The enhancement of Zn uptake in Cd-treated plants may indicate that the plants actively defend themselves against Cd binding to essential Zn sites by shifting the metal equilibrium toward Zn. A similar interaction has been observed earlier (Küpper et al., 2000, 2001) between Mg and toxic metals, such as Cd and Ni.

The high Cd uptake efficiency of the Ganges ecotype allowed for a detailed analysis of the ligand types around Cd in plant samples. Furthermore, the measurement of the Zn K edge EXAFS in the same samples helped to compare the affinity of both metals for the ligands available in these plants.

Processing of XAS/EXAFS Data of Intact Tissues

The Zn ligand distances reported here (2.05–2.07 Å) fit very well with distances published for plant samples by Salt et al. (1999) and reported for model compounds and high resolution protein crystal structures (Zn-His, approximately 2.00 Å; and Zn-O, 1.95–2.14 Å; Harding, 2001). For the Cd ligation, no comprehensive reference study is available, but the distances reported here (Cd-S, 2.46–2.50 Å; and Cd-N/O, 2.25–2.31 Å) match the values published by Salt et al. (1995) for plant samples and typical values in the Cambridge Structural Database for model systems with similar metal environment (Cd-S, 2.46–2.60 Å; and Cd-N/O, 2.22–2.40 Å) and values published by Dakanali et al. (2003) for Cd-citrate. The values found for the Fermi energy are in general agreement with the literature (for Zn, Clark-Baldwin et al., 1998; and for Cd, Pickering et al., 1999), except for the Cd mature petioles. The ligand proportions and distances of this data set were nevertheless in the normal range (for plant material, see Salt et al., 1995) and very similar to the physiologically related sample of the mature petioles.

Because XAS integrates over all existing sites of the element under study, the measured EXAFS patterns resembled a superposition of different metal-binding

Table II. *Results of the refinement of the EXAFS spectra using the Excurve98 program*

The graphs of the fits for young leaves are shown in Figures 2 and 3, and those of all other samples are displayed in the figures of the supplemental material. For the samples Zn His and Cd glutathione, the lower no. of ligands results in a slightly better FI. On the basis of an EXAFS analysis, the difference between five and six ligands cannot be distinguished. Similarly, when two different distances were refined for O and N, no significant improvement was found. EF, Fermi energy, defines the threshold for the EXAFS spectra (Rehr and Albers, 2000). This value was refined for every sample. SE, Mathematical SEs of the refinement (two sigma level). The error of the EXAFS approach as such is higher, about 10% for the proportions, 1 for the no. of total ligands, and 0.01 Å for the interatomic distances. This is revealed by the differences between samples of the same type, shown here for the Cd edge of young and mature leaves, 100 μM Cd + 10 μM Zn.

Sample	No. of Ligands (±SE)	Distance (±SE)	σ_i^2 (±SE)	EF (±SE)	FI × k^3 (±SE)
		Å	Å²		
Zn K edge					
Young leaves, 100 μM Cd + 10 μM Zn	4.1 (±0.3) O 1.9 (± 0.3) His	2.069 (±0.004)	0.0070 (±0.004)	9669.7 (±0.5)	0.30
Mature leaves, 100 μM Cd + 10 μM Zn	4.2 (±0.4) O 1.8 (±0.4) His	2.069 (±0.004)	0.0064 (±0.004)	9669.5 (±0.6)	0.39
Mature leaves, 0 μM Cd + 10 μM Zn	4.1 (±0.5) O 1.9 (± 0.5) His	2.050 (±0.006)	0.0082 (±0.006)	9669.2 (±0.7)	0.63[a]
Dead leaves, 100 μM Cd + 10 μM Zn	2.5 (±0.3) O 3.5 (± 0.3) His	2.049 (±0.006)	0.0110 (±0.006)	9668.8 (±0.6)	0.50
Mature petioles, 100 μM Cd + 10 μM Zn	3.4 (±0.4) O 2.6 (±0.4) His	2.070 (±0.005)	0.0085 (±0.005)	9669.0 (±0.6)	0.44
Mature stems, 100 μM Cd + 10 μM Zn	2.9 (±0.4) O 3.1 (±0.4) His	2.056 (±0.006)	0.0093 (±0.006)	9669.0 (±0.7)	0.56
Mature stems, 0 μM Cd + 10 μM Zn	2.9 (±0.9) O 3.1 (±0.9) His	2.060 (±0.013)	0.0092 (±0.012)	9669.0 (±1.3)	1.09[a]
Cd K edge					
Young leaves, 100 μM Cd + 10 μM Zn	1.5 S 4.5 (±0.2) N/O	2.51 (±0.01) 2.28 (±0.01)	0.008 (±0.0005)	26,714.7 (±0.8)	0.16
See above, second sample	1.6 S 4.4 (±0.4) N/O	2.49 (±0.006) 2.29 (±0.01)	0.009 (±0.0005)	26,716.0 (±1.5)	0.26
Mature leaves, 100 μM Cd + 10 μM Zn	1.5 S 4.5 (±0.3) N/O	2.50 (±0.01) 2.28 (±0.01)	0.010 (±0.0005)	26,714.9 (±1.1)	0.29
See above, second sample	1.1 S 4.9 (±0.2) N/O	2.43 (±0.01) 2.32 (±0.005)	0.010 (±0.0005)	26,717.8 (±0.7)	0.34
Mature leaves, 50 μM Cd + 10 μM Zn	1.4 S 4.6 (±0.3) N/O	2.46 (±0.02) 2.31 (±0.01)	0.011 (±0.001)	26,716.8 (±1.4)	0.42
Senescent leaves, 100 μM Cd + 10 μM Zn	0.3 S 5.7 (±0.4) N/O	2.47 (±0.07) 2.28 (±0.01)	0.007 (±0.0005)	26,717.1 (±1.7)	0.74
Dead leaves, 100 μM Cd + 10 μM Zn	0.7 S 5.3 (±0.3) N/O	2.49 (±0.02) 2.29 (±0.01)	0.010 (±0.0005)	26,716.0 (±1.0)	0.42
Mature petioles, 100 μM Cd + 10 μM Zn	3.1 S 2.9 (±0.1) N/O	2.49 (±0.01) 2.25 (±0.01)	0.010 (±0.0005)	26,711.0 (±0.7)	0.53
Senescent petioles, 100 μM Cd + 10 μM Zn	0.9 S 5.1 (±0.2) N/O	2.49 (±0.010) 2.29 (±0.006)	0.008 (±0.0005)	26,717.2 (±0.8)	0.18
Mature stems, 100 μM Cd + 10 μM Zn	2.3 S 3.7 (±0.3) N/O	2.50 (±0.01) 2.28 (±0.01)	0.009 (±0.0005)	26,713.2 (±1.3)	0.23
Senescent stems, 100 μM Cd + 10 μM Zn	1.5 S 4.5 (±0.5) N/O	2.49 (±0.01) 2.29 (±0.01)	0.010 (±0.0005)	26,715.9 (±1.7)	0.42

[a] FI is higher due to the lower signal to noise ratio of the measured data.

sites in various cells and subcellular compartments. Note that both fitting approaches yielded identical results concerning the main ligands, although they are based on different simplifying assumptions. The refinement with Excurve98 simulates the interaction between the central ion and mimics of its ligands. Thus, only individual atoms are modeled but not any interactions (steric hindrance, etc.) between parts of the same ligand and between neighboring ligands around the central ion. In contrast, the measured spectra of the model compounds mimic the set of ligands under natural conditions. Fitting XAS data as a linear combination of measured model data is based on the assumption that each subcellular compartment (e.g. vacuole, cytoplasm, chloroplasts, cell wall) of each cell has only one characteristic type of ligands (e.g. thiols, organic acids, or His). Only in this case can the interaction between different types of ligands, which would lead to changes in metal-ligand bond lengths, be ignored.

Table III. *Results of fitting the XAS spectra (energy region of the EXAFS analysis, i.e. 20 to 500 eV above the edge) with a linear combination of the measured data sets of representative model compounds*

The graphs of the fits for young leaves are shown in Figures 2 and 3. Those of all other samples are displayed in the figures of the supplemental material. SE, Mathematical SEs of fit (one sigma level). The error of the method as such is higher due to systematic errors; also, the variability of the plants has to be kept in mind. Both contribute to the differences between samples of the same type, as shown for the Cd edge of young and mature leaves, 100 μM Cd + 10 μM Zn. –, Not measured.

Sample	Cd ligands (±SE; Cd edge measurement)	Zn ligands (±SE; Zn edge measurement)
Young leaves, 100 μM Cd + 10 μM Zn	20% (±3%) His 46% (±3%) O ligands[a] 35% (±1%) S ligands[b]	20% (±3%) His 80% (±2%) O ligands[a]
See above, second sample	10% (±5%) His 56% (±4%) O ligands[a] 34% (±1%) S ligands[b]	–
Mature leaves, 100 μM Cd + 10 μM Zn	28% (±3%) His 38% (±2%) O ligands[a] 34% (±1%) S ligands[b]	1% (±3%) His 99% (±2) O ligands[a]
See above, second sample	26% (±6%) His 54% (±5%) O ligands[a] 21% (±2%) S ligands[b]	–
Mature leaves, 50 μM Cd + 10 μM Zn	13% (±6%) His 63% (±5%) O ligands[a] 24% (±2%) S ligands[b]	–
Mature leaves, 0 μM Cd + 10 μM Zn	–	40% (±5%) His 60% (±3%) O ligands[a]
Senescent leaves, 100 μM Cd + 10 μM Zn	25% (±5%) His 59% (±5%) O ligands[a] 16% (±2%) S ligands[b]	–
Dead leaves, 100 μM Cd + 10 μM Zn	39% (±3%) His 30% (±3%) O ligands[a] 31% (±1%) S ligands[b]	70% (±3%) His 30% (±2%) O ligands[a]
Mature petioles, 100 μM Cd + 10 μM Zn	0% (±6%) His 75% (±5%) O ligands[a] 25% (±2%) S ligands[b]	34% (±5%) His 66% (±3%) O ligands[a]
Senescent petioles, 100 μM Cd + 10 μM Zn	11% (±5%) His 70% (±5%) O ligands[a] 20% (±2%) S ligands[b]	–
Mature stems, 100 μM Cd + 10 μM Zn	27% (±3%) His 36% (±2%) O ligands[a] 37% (±1%) S ligands[b]	38% (±4%) His 62% (±3%) O ligands[a]
Mature stems, 0 μM Cd + 10 μM Zn	–	46% (±6%) His
Senescent stems, 0 μM Cd + 10 μM Zn	3% (±4%) His 68% (±4%) O ligands[a] 29% (±1%) S ligands[b]	–

[a] No significant difference between the EXAFS spectra of organic acid and aqueous complexes were found; therefore, an average of both data sets was used as model for fitting. [b] The Cd-glutathione complex was used as model.

Metal Speciation and Detoxification in Hyperaccumulators

The present study documents that in the locations of the highest heavy metal concentrations in hyperaccumulator plants (>300 mM Zn is accumulated in the epidermal vacuoles of mature leaves; Küpper et al., 1999), most of the heavy metals are not bound by strong ligands. This makes sense from an energetical point of view. It is most likely cheaper for the plant to pump the metals into the epidermal vacuoles (Küpper et al., 1999) and store them there just weakly bound by organic acids that also act as counterions rather than investing energy for synthesizing the large amounts of strong ligands that would be required for binding the metal. The situation is different in nonaccumulator plants, where Cd is bound by S ligands (Cobbett and Goldsbrough, 2002). For such plants, it seems preferable to synthesize a ligand that can detoxify a range of metals compared with expressing a transporter protein that is specific for one or only a few metals.

An earlier study on metal compartmentation in *T. caerulescens* (Küpper et al., 1999) showed that young leaves generally contain less metal than adult leaves. Young leaves have a less pronounced sequestration in the epidermal vacuoles and a higher proportion of the total metal in the mesophyll (i.e. the photosynthetically active tissue). The present results may in-

dicate that in young leaves, it is advantageous for the plant to detoxify the heavy metals by synthesizing strong ligands until the sequestration in the vacuole becomes the main detoxification mechanism. Alternatively, it is possible that the mesophyll with its metal-sensitive photosynthetic apparatus (Prasad and Strzałka, 1999) is always protected against detoxification of heavy metals with strong ligands, whereas the metals in the epidermis are always stored as free ions or weak organic acid complexes in the vacuoles. The decrease of the proportion of strong ligands with increasing leaf age could then be explained by the increasing proportion of the total metal that is sequestered in the epidermal vacuoles as shown by Küpper et al. (1999). If EXAFS of frozen hydrated samples with single-cell resolution (Sarret et al., 2002; Pickering et al., 2003) will become more available in the future, it should be possible to distinguish between these two possibilities.

An increase in His complexation of both Cd and Zn was observed in senescent and dead leaves compared with young and mature leaves. This could be caused by the loss of the normal intracellular compartmentation in a dying leaf, allowing interaction of the metals normally stored in the vacuole (Vázquez et al., 1994; Küpper et al., 1999, 2001) with cytoplasmic components. Thus, heavy metals will not only bind to free His that is used for metal transport and detoxification (Krämer et al., 1996) but also to His residues of proteins. Furthermore, enhanced binding to chlorophyll (Küpper et al., 1996, 1998, 2002) will occur, which should lead to similar EXAFS signals as in the case of His coordination. The difference in metal speciation between dead and living tissues clearly demonstrates the necessity to preserve intracellular compartmentation (an approach also used by Salt et al., 1995), i.e. to avoid any fixation other than rapid freezing of hydrated tissues. Drying or freeze-thaw cycles would inevitably lead to an exchange of ligands because the metals that are normally stored in the vacuole (e.g. Küpper et al., 1999) would enter the cytoplasm and chloroplasts. Work on Ni in *Thlaspi goesingense* by Krämer et al. (2000), using cell fractionation and XANES to determine Ni compartmentation and speciation, suggested that the majority of Ni in leaves of the hyperaccumulator was associated with the cell wall. In contrast, Küpper et al. (2001), who used energy dispersive x-ray microanalysis of frozen hydrated tissues, found the vacuole to be the major compartment of Ni sequestration in Brassicaceae including *T. goesingense*. The discrepancy might be because Krämer et al. (2001) used a XANES spectrum of Ni-soaked cell wall material for fitting the XANES spectrum of the intact frozen cells. XANES/EXAFS yields information about the immediate metal environment and not about intracellular compartmentation. The cell wall mainly contains O ligands like carboxyl and hydroxyl groups, so it might not be distinguished properly from other O ligands. This limitation is well known from investigations on metalloenzymes. The second method applied by Krämer et al. (2000) was measuring the metals in isolated protoplasts/vacuoles and assigning all the remaining metal, which was measured in the samples before the preparation procedure, to the "apoplast". Here, originally intracellular metal might be released from the protoplasts/vacuoles (also the seemingly intact ones) during isolation.

The high ratio of His ligands around Zn and S ligands around Cd in stems may indicate that both Zn and Cd are transported as stable complexes, His in the case of Zn and phytochelatins or metallothioneins in the case of Cd. This would be in line with earlier data from Ni hyperaccumulator plants, where Krämer et al. (1996) have shown that free His is a transport ligand for Ni, complexing about 20% of the Ni in the xylem of these plants. On the other hand, Salt et al. (1999) did not find any His complexing Zn in xylem exudate of *T. caerulescens*, making an alternative explanation for the results of the present study more likely. It seems that at least part of this tissue-specific difference can be explained by the differing volumes of metal-storing compartments. The lower percentage of weak metal complexes in stems and petioles compared with leaves may be caused by a lower ratio of epidermal vacuole volume (and, therefore, amount of metal) in comparison with the total tissue volume. Our finding of about 24% to 30% His coordination of Zn in mature leaves is also in line with Salt et al. (1999), who found 16% His coordination in mature shoots (which are in *T. caerulescens* mainly leaves). Salt et al. (1999) did not analyze, however, petioles, stems, or young leaves, i.e. those tissues that we found to have a much higher ratio of Zn coordination by His.

In contrast to Cd, S ligands were not found to be involved in Zn complexation. This confirms the earlier studies of Salt et al. (1999) that used only mature tissues and of Sarret et al. (2002) who used the Zn hyperaccumulator *Arabidopsis halleri*. In our opinion, this can be explained mainly by two reasons. (1) According to Satofuka et al. (2001), phytochelatins have a much lower affinity for Zn compared with Cd. Thus, under limited concentrations of phytochelatins, mostly Cd will be coordinated. However, this cannot be the major reason because samples from plants without any Cd did not have any S ligands around Zn. (2) In the case of Zn, S ligands are not required because the sequestration of Zn in the vacuoles plus the complexation by His provide sufficient protection from the very beginning of leaf ontogenesis. Therefore, if only Zn is supplied to the plant, phytochelatins will not be expressed. This is in line with the observation that there is not any correlation between the content of Zn and S in the cells of Zn hyperaccumulator plants (Küpper et al., 1999, 2000).

MATERIALS AND METHODS

Plant Material, Culture Media, and Culture Conditions

Seeds of *Thlaspi caerulescens* J.&C. Presl, Ganges ecotype, were germinated on a mixture of perlite and vermiculite moistened with deionized water. Three weeks after germination, seedlings were transferred to 1.5-L vessels filled with a solution containing 1,000 μM $Ca(NO_3)_2$, 500 μM $MgSO_4$, 50 μM K_2HPO_4, 100 μM KCl, 10 μM H_3BO_3, 1.8 μM $MnSO_4$, 0.2 μM Na_2MoO_4, 0.31 μM $CuSO_4$, 0.5 μM $NiSO_4$, 20 μM Fe(III)-EDDHA (Fe(III)-ethylenediamine-di(o-hydroxyphenylacetic acid), and 10 μM $ZnSO_4$ (Shen et al., 1997). The pH of the solution was maintained at around 6.0 with 2,000 μM MES (50% as potassium salt). The nutrient solution was aerated continuously and renewed every 5 d. Two weeks after transferring the seedlings into hydroponic solution, 0 (control), 50, or 100 μM $CdSO_4$ was added to the solution. Each treatment was replicated with two pots (each of them with four plants) in a first experiment and with one pot (four plants) in a second experiment half a year later.

Plants were grown in a room with 14-h day length and 24°C/20°C day/night temperature. The photon flux density during the light period was 60 μmol m^{-2} s^{-1}. Irradiance was supplied by a 1:1 mixture of "cool-white" and Osram Fluora fluorescent tubes (Osram, München, Germany).

Preparation of Plant Samples for EXAFS Measurements

After about 6 months of plant growth, samples were taken from several plant organs (stems, leaf petioles, and leaves). To eliminate problems of element redistribution during sample preparation, the collected tissues were frozen in melting N slush and afterwards immediately stored at −80°C. To obtain representative data sets within the limited Synchrotron beam time, aliquots of samples from all plants of the same metal treatment (see above) were mixed, so that each EXAFS sample represented the average of four to eight plants. For the EXAFS measurements, the frozen hydrated samples were ground to powder in a mortar and filled into EXAFS cuvettes; this was also all done at −80°C. Afterward, the cuvettes were sealed with Kapton tape (Kaptontape, Torrance, CA) and stored in liquid N.

Preparation of Model Complexes for EXAFS Measurements

Five millimolar solutions of both Zn and Cd sulfate were used as reference for the aquo complexes. His and glutathione complexes of both metals were made by adding 50 mM ligand to a 5 mM solution of the metal sulfates. The Cd citrate complex was made by adding 50 mM citric acid to an aqueous solution of 5 mM $CdSO_4$; Zn citrate was obtained from Merck (Darmstadt, Germany) and dissolved in 50 mM citric acid. Our model complexes were acidic, resembling the situation in plant vacuoles, which are the compartments where plants store organic acids and are main sinks for heavy metals in hyperaccumulators (Küpper et al., 1999, 2001). The pH values were about 2.6 for the citrate complexes, 2.9 for the glutathione complexes, 4.8 for the aquo complexes, and 6.0 for the His complexes. All solutions of the model complexes contained 30% (v/v) glycerol to minimize the formation of ice crystals during freezing. The samples were transferred into EXAFS cuvettes and frozen in liquid N.

EXAFS Measurements and Data Analysis

Measurements were performed at the EMBL bending magnet beam line D2 (DESY, Hamburg, Germany) using for the Zn K edge an Si(111) and for the Cd K edge an Si(311) double crystal monochromator, a focusing mirror (for Zn only), and a 13-element Ge solid-state fluorescence detector. All samples were mounted in a top-loading closed-cycle cryostat (modified Oxford Instruments, Wiesbaden, Germany) and kept at about 30 K. The transmitted beam was used for energy calibration by means of the Bragg reflections of a static Si(220) crystal (Pettifer and Hermes, 1985). Between 1 and 2 million counts per data point above the absorption edge were accumulated for each Cd edge measurement, and at least 500,000 counts were accumulated for each Zn edge measurement.

The EXPROG program package (Hermes and Nolting, EMBL, Hamburg) was employed for data reduction. Analysis of the spectra was done with Excurve98 using constrained parameters (Binstead et al., 1992) with a data range from k = 2.0 $Å^{-1}$ to k = 13.5 $Å^{-1}$ for the Zn K edge and from k = 3.0 $Å^{-1}$ to k = 12.5 $Å^{-1}$. The set of potential ligands coordinating Zn and Cd is limited to S, O, and N for these samples. EXAFS data analysis generally cannot discriminate between N and O ligation. However, aromatic ligands, such as His, can be identified via the specific multiple scattering pattern they generate. For the imidazole ring with one N at about 2 Å, two C at about 3 Å, and an N and an C at about 4 Å, multiple scattering contributions up to 5th order were considered in the simulations. All other contributions were calculated in the single scattering small atom approximation (Rehr and Albers, 1990). The distance of N and O ligands were kept at identical distances for the refinement to lower the number of free parameters and to prevent overinterpretation of data. For Cd, the multiple scattering contributions from imidazoles are not significant. Even in the case of proteins where the coordination of His is known (Heinz et al., 2003), multiple scattering contributions are difficult to refine. S contributions to the first shell at around 2.5 Å are clearly distinct from those of low Z scatterers. As a consequence, for the Excurve refinement only one shell for low Z scatterers (N/O) and one for S scatterers were included. In this case, the His contribution was estimated only by the CA (see below). For all spectra, the Fermi energy, the first shell distances, the Debye-Waller parameters, and the coordination numbers of the potential ligands were refined. The Fermi energy defines the energy threshold of each EXAFS spectrum (Rehr and Albers, 2000). The Debye-Waller parameter is proportional to static and dynamic disorder of each shell. The bond distances obtained for the metal coordination in plant compartments are consistent with the distances determined for the model systems (see Table II). This consistency is indirect proof for the approach we used.

In addition to the refinement described above, the measured data of all plant samples were fitted with a linear combination of the measured curves of all model complexes. This fit, subsequently called CA, was done to have a second method to estimate the proportions of the different types of ligands around the metals. No k weighting was applied to data lowering the influence of noise at high photoelectron wave vector (k). The fitting of measured XAS sample data by a linear combination of measured model data has also been used successfully by Salt et al. (1999) for Zn in samples of *T. caerulescens*. In the present work, the approach of Salt et al. was modified as follows. In the present work, the EXAFS range of energies (i.e. 20–500 eV above the edge) was fitted instead of the extended XANES range used by Salt et al. This was done because the SES of the fits and also the deviations between samples of the same tissue were much larger for the XANES region (data not shown) compared with the EXAFS region (Table III). This had to be expected because in the XAS spectra of the XANES region, the visible differences between the model compounds were also much smaller than in the EXAFS region (Fig. 1, top), so that tiny differences in normalization of the spectra could strongly affect the results. In addition, because of the steepness of the edge, already small (1–2 eV) inaccuracies in the energy calibration of the spectra lead to large errors in the CA around the edge. Therefore, only the data of the EXAFS region were used for further analysis. Because the XAS and EXAFS spectra of the aqueous and organic acid complexes of both metals were not sufficiently different to distinguish between them with an acceptable error margin (Fig. 1), we averaged these two model complexes in the fits of the plant samples.

Determination of Metals in Whole-Plant Tissues

Frozen hydrated plant samples (see above) were lyophilized, ground, and subsequently digested with a mixture of HNO_3 and $HClO_4$ (Zhao et al., 1994). Concentrations of Cd and Zn in the digests were determined using inductively coupled plasma mass spectroscopy.

ACKNOWLEDGMENTS

We are very grateful to Ivan Šetlík for stimulating discussions and in raising the plants and setting up the conditions for their growth. The authors thank Dr. Thomas Meyer for extracting reference data on Cd ligation from the Cambridge Structural Database. We would like to thank Anna Ruprechtová and Marie Šimková for germination of the seeds.

Received September 4, 2003; returned for revision September 24, 2003; accepted November 11, 2003.

LITERATURE CITED

Baker AJM (1981) Accumulators and excluders-strategies in the response of plants to heavy metals. J Plant Nutr **3:** 643–654

Baker AJM, Brooks RR (1989) Terrestrial higher plants which hyperaccumulate metallic elements: a review of their distribution, ecology and phytochemistry. Biorecovery **1:** 81–126

Barón M, Arellano JB, Gorge JL (1995) Copper and photosystem II: a controversial relationship. Physiol Plant **94:** 174–180

Binstead N, Strange RW, Hasnain SS (1992) Constrained and restrained refinement in EXAFS data analysis with curved wave theory. Biochemistry **31:** 12117–12125

Boyd RS (1998) Hyperaccumulation as a plant defence strategy. *In* Brooks RR, ed, Plants That Hyperaccumulate Heavy Metals. CAB International, Wallingford, UK, pp 181–201

Brooks RR, Lee J, Reeves RD, Jaffre T (1977) Detection of nickeliferous rocks by analysis of herbarium species of indicator plants. J Geochem Explor **7:** 49–57

Brooks RR (1998) Geobotany and hyperaccumulators. *In* RR Brooks, ed, Plants That Hyperaccumulate Heavy Metals. CAB International, Wallingford, UK, pp 55–94

Clark-Baldwin K, Tierney DL, Govindaswamy N, Gruff ES, Kim Ch, Berg J, Koch SA, Penner-Hahn JE (1998) The limitations of X-ray absorption spectroscopy for determining the structure of zinc sites in proteins: when is a tetrathiolate not a tetrathiolate? J Am Chem Soc **120:** 8401–8409

Clijsters H, Van Assche F (1985) Inhibition of photosynthesis by heavy metals. Photosynth Res **7:** 31–40

Cobbett C, Goldsbrough P (2002) Phytochelatins and metallothioneins: roles in heavy metal detoxification and homeostasis. Annu Rev Plant Biol **53:** 159–182

Dakanali M, Kefalas ET, Raptopoulou CP, Terzis A, Mavromoustakos T, Salifoglou A (2003) Synthesis and spectroscopic and structural studies of a new cadmium(II)-citrate aqueous complex: potential relevance to cadmium(II)-citrate speciation and links to cadmium toxicity. Inorg Chem **42:** 2531–2537

Ebbs S, Lau I, Ahner B, Kochian LV (2002) Phytochelatin synthesis is not responsible for Cd tolerance in the Zn/Cd hyperaccumulator *Thlaspi* (J.&C. Presl). Planta **214:** 635–640

Fernandes JC, Henriques FS (1991) Biochemical, physiological and structural effects of excess copper in plants. Bot Rev **57:** 246–273

Frey B, Keller C, Zierold K, Schulin R (2000) Distribution of Zn in functionally different epidermal cells of the hyperaccumulator *Thlaspi caerulescens*. Plant Cell Environ **23:** 675–687

Harding MM (2001) Geometry of metal-ligand interactions in proteins. Acta Cryst **D57:** 401–411

Heinz U, Bauer R, Wommer S, Meyer-Klaucke W, Papamichaels C, Bateson J, Adolph HW (2003) Coordination geometries of metal ions in D- or L-captopril-inhibited metallo-beta-lactamases. J Biol Chem **278:** 20659–20666

Krämer U, Cotterhowells JD, Charnock JM, Baker AJM, Smith JAC (1996) Free histidine as a metal chelator in plants that accumulate nickel. Nature **379:** 635–638

Krämer U, Pickering IJ, Prince RC, Raskin I, Salt DE (2000) Subcellular localization and speciation of nickel in hyperaccumulator and non-accumulator *Thlaspi* species. Plant Physiol **122:** 1343–1353

Küpper H, Küpper F, Spiller M (1996) Environmental relevance of heavy metal substituted chlorophylls using the example of water plants. J Exp Bot **47:** 259–266

Küpper H, Küpper F, Spiller M (1998) In situ detection of heavy metal substituted chlorophylls in water plants. Photosynth Res **58:** 125–133

Küpper H, Lombi E, Zhao FJ, McGrath SP (2000) Cellular compartmentation of cadmium and zinc in relation to other elements in the hyperaccumulator *Arabidopsis halleri*. Planta **212:** 75–84

Küpper H, Lombi E, Zhao FJ, Wieshammer G, McGrath SP (2001) Cellular compartmentation of nickel in the hyperaccumulators *Alyssum lesbiacum*, *Alyssum bertolonii* and *Thlaspi goesingense*. J Exp Bot **52:** 2291–2300

Küpper H, Šetlík I, Spiller M, Küpper FC, Prášil O (2002) Heavy metal-induced inhibition of photosynthesis: targets of in vivo heavy metal chlorophyll formation. J Phycol **38:** 429–441

Küpper H, Zhao FJ, McGrath SP (1999) Cellular compartmentation of zinc in leaves of the hyperaccumulator *Thlaspi caerulescens*. Plant Physiol **119:** 305–311

Lane TW, Morel FMM (2000) A biological function for cadmium in marine diatoms. Proc Natl Acad Sci USA **97:** 4627–4631

Lombi E, Zhao FJ, Dunham SJ, McGrath SP (2000) Cadmium accumulation in populations of *Thlaspi caerulescens* and *Thlaspi goesingense*. New Phytol **145:** 11–20

Lombi E, Zhao FJ, McGrath SP, Young SD, Sacchi GA (2001) Physiological evidence for a high-affinity cadmium transporter highly expressed in a *Thlaspi caerulescens* ecotype. New Phytol **149:** 43–60

Maeda S, Sakaguchi T (1990) Accumulation and detoxification of toxic metal elements by algae. *In* I Akatsuka I, ed, Introduction to Applied Phycology. SPB Academic Publishing, The Hague, The Netherlands, pp 109–136

McGrath SP, Sidoli CMD, Baker AJM, Reeves RD (1993) The potential for the use of metal-accumulating plants for the in situ decontamination of metal-polluted soils. *In* HJP Eijsackers, T Hamers, eds, Integrated Soil and Sediment Research: A Basis for Proper Protection. Kluwer Academic Publishers, Dordrecht, The Netherlands, pp 673–677

McGrath SP, Zhao FJ, Lombi E (2002) Phytoremediation of metals, metalloids, and radionuclides. Adv Agron **75:** 1–56

Pence NS, Larsen PB, Ebbs SD, Letham DLD, Lasat MM, Garvin DF, Eide D, Kochian LV (2000) The molecular physiology of heavy metal transport in the Zn/Cd hyperaccumulator *Thlaspi caerulescens*. Proc Natl Acad Sci USA **97:** 4956–4960

Pettifer RF, Hermes C (1985) Absolute energy calibration of X-ray radiation from synchrotron sources. J Appl Crys **18:** 404–412

Pickering IJ, Hirsch G, Prince RC, Sneeden EY, Salt DE, George GN (2003) Imaging of selenium in plants using tapered metal monocapillary optics. J Synchrotron Rad **10:** 289–290

Pickering IJ, Prince RC, George GN, Rauser WE, Wickramasinghe WA, Watson AA, Dameron CT, Dance IG, Fairlie DP, Salt DE (1999) X-ray absorption spectroscopy of cadmium phytochelatin and model systems. Biochim Biophys Acta **1429:** 351–364

Prasad MNV, Hagemeyer J (eds.) (1999) Heavy Metal Stress in Plants: from Molecules to Ecosystems. Springer, Berlin

Prasad MNV, Strzałka K (1999) Impact of heavy metals on photosynthesis. *In* MNV Prasad, J Hagemeyer, eds, Heavy Metal Stress in Plants: from Molecules to Ecosystems. Springer, Berlin, pp 117–128

Psaras GK, Constantinidis TH, Cotsopoulos B, Manetas Y (2000) Relative abundance of nickel in the leaf epidermis of eight hyperaccumulators: evidence that the metal is excluded from both guard cells and trichomes. Ann Bot **86:** 73–88

Psaras GK, Manetas Y (2001) Nickel localization of the metal hyperaccumulator *Thlaspi pindicum* Hausskn. Ann Bot **88:** 513–516

Rehr JJ, Albers RC (1990) Scattering-matrix formulation of curved-wave multiple-scattering theory: application to X-ray-absorption fine structure. Phys Rev B **41:** 8139–8149

Rehr JJ, Albers RC (2000) Theoretical approaches to x-ray absorption fine structure. Rev Mod Phys **72:** 621–654

Robinson BH, Leblanc M, Petit D, Brooks RR, Kirkman JH, Gregg PEH (1998) The potential of *Thlaspi caerulescens* for phytoremediation of contaminated soils. Plant Soil **203:** 47–56

Salt DE, Prince RC, Pickering IJ, Raskin I (1995) Mechanisms of cadmium mobility and accumulation in Indian mustard. Plant Physiol **109:** 1427–1433

Salt DE, Prince RC, Baker AJM, Raskin I, Pickering IJ (1999) Zinc ligands in the metal hyperaccumulator *Thlaspi caerulescens* as determined using X-ray absorption spectroscopy. Environ Sci Technol **33:** 712–717

Sarret G, Saumitou-Laprade P, Bert V, Proux O, Hazemann JL, Traverse A, Marcus MA, Manceau A (2002) Forms of zinc accumulated in the hyperaccumulator *Arabidopsis halleri*. Plant Physiol **130:** 1815–1826

Satofuka H, Fukui T, Takagi M, Atomi H, Imanaka T (2001) Metal-binding properties of phytochelatin-related peptides. J Inorg Biochem **86:** 595–602

Shen ZG, Zhao FJ, McGrath SP (1997) Uptake and transport of zinc in the hyperaccumulator *Thlaspi caerulescens* and the non-hyperaccumulator *Thlaspi ochroleucum*. Plant Cell Environ **20:** 898–906

van Hoof NALM, Koevoets PLM, Hakvoort HWJ, Ten Bookum WM, Schat H, Verkleij JAC, Ernst WHO (2001) Enhanced ATP-dependent copper efflux across the root cell plasma membrane in copper-tolerant *Silene vulgaris*. Physiol Plant **113:** 225–232

Vázquez MD, Poschenrieder C, Barceló J, Baker AJM, Hatton P, Cope GH (1994) Compartmentation of zinc in roots and leaves of the zinc hyperaccumulator *Thlaspi caerulescens* J & C Presl. Bot Acta **107:** 243–250

Zhao FJ, Evans EJ, Bilsborrow PE, Syers JK (1994) Influence of nitrogen and sulfur on the glucosinolate profile of rapeseed (*Brassica napus* L.). J Sci Food Ag **64:** 295–304